Doublet bands in ^{126}Cs in the triaxial rotor model coupled with two quasiparticles

S. Y. Wang,[1] S. Q. Zhang,[1,2,*] B. Qi,[1] and J. Meng[1,2,3,†]

[1]*School of Physics, and MOE Key Laboratory of Heavy Ion Physics, Peking University, Beijing 100871, China*

[2]*Institute of Theoretical Physics, Chinese Academy of Science, Beijing 100080, China*

[3]*Center of Theoretical Nuclear Physics, National Laboratory of Heavy Ion Accelerator, Lanzhou 730000, China*

(Dated: February 9, 2008)

Abstract

The positive parity doublet bands based on the $\pi h_{11/2} \otimes \nu h_{11/2}$ configuration in ^{126}Cs have been investigated in the two quasi-particles coupled with a triaxial rotor model. The energy spectra $E(I)$, energy staggering parameter $S(I) = [E(I) - E(I-1)]/2I$, $B(M1)$ and $B(E2)$ values, intraband $B(M1)/B(E2)$ ratios, $B(M1)_{\rm in}/B(M1)_{\rm out}$ ratios, and orientation of the angular momentum for the rotor as well as the valence proton and neutron are calculated. After including the pairing correlation, good agreement has been obtained between the calculated results and the data available, which supports the interpretation of this positive parity doublet bands as chiral bands.

PACS numbers: 21.10.Re, 21.60.Cs, 21.60.Ev

*e-mail: sqzhang@pku.edu.cn

†e-mail: mengj@pku.edu.cn

I. INTRODUCTION

Since the original 1997 work of Frauendorf and Meng [1], the phenomenon of chiral rotation in atomic nuclei has attracted significant attention. Lots of experimental and theoretical efforts have been devoted to search for [2, 3, 4, 5, 6, 7, 8, 9, 10, 11, 12, 13, 14, 15, 16] and to interpret [17, 18, 19, 20, 21, 22, 23] this phenomenon.

Following the scenario that the chiral doublet bands are expected to occur in the mass region where the proton (or neutron) Fermi surface lies at the bottom of the high-j subshell and the neutron (or proton) Fermi surface lies at the top of the high-j subshell, there have been a number of experimental studies searching for chiral doublet bands in the $A \sim$130 and 100 region. For $A \sim$130 region, candidate chiral bands have been proposed in $N = 77$ (^{132}Cs, ^{134}La) [6, 10], $N = 75$ (^{130}Cs, ^{132}La, ^{134}Pr, ^{136}Pm, ^{138}Eu) [2, 4, 5, 7], $N = 73$ (^{128}Cs, ^{130}La, ^{132}Pr) [3, 16] , and $N = 71$ (^{126}Cs) [8, 13] isotones.

The observation of the chirality in ^{126}Cs, ^{128}Cs, ^{130}Cs, ^{132}Cs provides a good opportunity to investigate the dependence of its occurrence on the number of the valence neutron in high-j shell. In particular, for Cs isotopes, the proton Fermi levels are supposed to lie in the lower $\pi h_{11/2}$ subshell, and compared with ^{130}Cs and ^{132}Cs where the neutron Fermi levels are supposed to lie in the upper $\nu h_{11/2}$ subshell, the neutron Fermi level in ^{126}Cs is likely close to be in the middle of the $\nu h_{11/2}$ subshell. Therefore it is interesting to examine the mechanism for the occurrence of the chirality in ^{126}Cs.

Motivated by these considerations, two quasi-particles coupled with a triaxial rotor model is employed for the analysis of the positive parity doublet bands in ^{126}Cs. The rotational energy spectra $E(I)$, energy staggering parameter $S(I) = [E(I) - E(I-1)]/2I$, $B(M1)$ and $B(E2)$ values, intraband $B(M1)/B(E2)$ ratios, $B(M1)_{\rm in}/B(M1)_{\rm out}$ ratios, and orientation of the angular momentum for the rotor as well as the valence proton and neutron will be investigated and compared with the data available. The interpretation of this positive parity doublet bands as chiral bands will be discussed.

II. MODEL

The particle-rotor model (PRM) has been extensively used in the investigation of the chiral rotation [1, 9, 19, 20, 21] due to the advantages of the good angular momentum and

simple picture. Compared with the conventional cranking approach, PRM is a quantum mechanical method which describes the system in the laboratory framework and yields directly the energy splitting and tunneling between doublet bands. In Refs.[1, 19], the PRM with one particle and one hole coupled with a triaxial rotor has been developed and used in the analysis of chiral bands. The PRM Hamiltonian is written as

$$\hat{H} = \hat{H}_{\rm core} + \hat{H}_{\rm p} + \hat{H}_{\rm n}, \tag{1}$$

where $\hat{H}_{\rm core}$ represents the Hamiltonian of the rotor,

$$\hat{H}_{\rm core} = \sum_{\nu=1}^{3} \frac{(I_\nu - j_{{\rm p}\nu} - j_{{\rm n}\nu})^2}{2\mathcal{J}_\nu}, \tag{2}$$

$\mathcal{J}_\nu (\nu = 1, 2, 3)$ is the irrotational moment of inertia,

$$\mathcal{J}_\nu = \mathcal{J} \sin^2(\gamma - \frac{2\pi}{3}\nu)(\nu = 1, 2, 3), \tag{3}$$

$H_{\rm p}$ and $H_{\rm n}$ describe the Hamiltonians of the single proton and neutron outside the rotor which for a single-j model can be given as,

$$H_{\rm p(n)} = \pm\frac{1}{2}C\left\{\cos\gamma\left(j_3^2 - \frac{j(j+1)}{3}\right) + \frac{\sin\gamma}{2\sqrt{3}}\left(j_+^2 + j_-^2\right)\right\} \tag{4}$$

where the plus sign refers to a particle and the minus to a hole and the coupling parameter C is proportional to the quadrupole deformation β.

Including the pairing by the standard BCS quasiparticle approximation, the PRM can be generalized to the two quasiparticles coupled with a triaxial rotor cases. The single-particle energies ϵ_ν obtained by diagonalizing the single proton (neutron) Hamiltonian in PRM [1, 19] are replaced with the corresponding quasiparticle energies E_ν,

$$E_{\nu i} = \sqrt{(\epsilon_{\nu i} - \lambda_i)^2 + \Delta_i^2}, \qquad\qquad i = {\rm n},\ {\rm p} \tag{5}$$

where $\varepsilon_{\nu i}$ is the single particle energies, Δ_i the pairing gaps and λ_i the Fermi energies. In comparison with the case excluding pairing, each single-particle matrix element needs to be multiplied by a pairing factor $u_\mu u_\nu + v_\mu v_\nu$ [24, 25], in which the pairing occupation factor v_ν of the state ν is given by

$$v_\nu^2 = \frac{1}{2}\left[1 - \frac{\epsilon_\nu - \lambda}{E_\nu}\right], \tag{6}$$

and $u_\nu^2 + v_\nu^2 = 1$. With inclusion of pairing, the present model goes beyond the one particle one hole coupled with the triaxial rotor model, and the configuration of multi-particles sitting in a high j-shell can be simulated by adjusting the Fermi level. The detailed formalism and numerical calculation will be published later [26].

III. RESULT AND DISCUSSION

Using the above two quasiparticles coupled with a triaxial rotor model, the doublet bands in ^{126}Cs has been investigated.

In the calculation, the quadrupole deformation $\varepsilon_2 = 0.244$ and $\gamma = 24^\circ$ are taken from Ref. [27]. However, similar as in other PRM calculations [21, 28], in order to achieve better agreement with the experimental energy spectra a slightly larger value is taken, i.e., $\varepsilon_2 = 0.26$. Accordingly, the parameter $C = 0.3$ MeV which corresponds to $\varepsilon_2 \simeq 0.26$ in the 130 mass region. The moment of inertia $\mathcal{J} = 20\ \hbar^2/\text{MeV}$ is determined by the slope of the experimental E versus I curve.

Following the empirical formula Δ=$12/\sqrt{A}$, the pairing gap $\Delta = 1.0$ MeV is used for both protons and neutrons. As mentioned above, as the valence proton in ^{126}Cs with $Z = 55$ and $N = 71$ is supposed to be at the beginning of the $\pi h_{11/2}$ sub-shell, the proton Fermi energy $\lambda_{\rm p}$ takes value of -2.293 MeV. The neutron Fermi energy $\lambda_{\rm n}$ takes value of 0.8 MeV which lies in the middle of the $\nu h_{11/2}$ sub-shell and simulates the effect of multi-valence neutrons. In the calculation of the electromagnetic transitions, the empirical intrinsic qudrupole moment $Q_0 = 3.5$ eb, gyromagnetic ratios $g_{\rm R} = Z/A \approx 0.44$, $g_{\rm p} = 1.21$ and $g_{\rm n} = -0.21$ have been adopted.

The calculated energy spectra $E(I)$ and the energy staggering parameter $S(I)$, defined as $[E(I) - E(I-1)]/2I$, for the doublet bands in ^{126}Cs are presented in Fig. 1, together with the corresponding experimental results. The calculated energy spectra well reproduce the experimental results, and show a constant energy separation of ~ 200 keV between the two bands at large spin interval $9\hbar \leq I \leq 18\hbar$. The energy staggering parameter $S(I)$ is indicative of the degree of mutual orthogonality of the three vectors involved. For ideal chiral bands, $S(I)$ should be spin independent [29]. In Fig. 1, it can be seen that the theoretical $S(I)$ values reproduce experimental one well. For $I \geq 18\hbar$, the theoretical $S(I)$ values overestimate the amplitude of staggering, which is due to the large Coriolis effect

at high spins. It can be expected that the attenuation of Coriolis effect may reduce the staggering discrepancy of $S(I)$.

It has been suggested in ref. [29] that the observed staggering of the ratios $B(M1)/B(E2)$ and $B(M1)_{\rm in}/B(M1)_{\rm out}$ (the subscript *in* and *out* represent respectively the intraband and interband) can be understood as signatures of the chiral bands. The calculated $B(M1)/B(E2)$ and $B(M1)_{\rm in}/B(M1)_{\rm out}$ values together with their corresponding experimental results for the doublet bands in ^{126}Cs are presented in the Fig. 2 and 3, respectively. It can be seen that the agreement for the $B(M1)/B(E2)$ ratios at the whole spin region is excellent. The magnitude, staggering and the decreasing trend of the ratios with spin are reproduced quite well. Furthermore the experimental staggering phase is exactly reproduced in the calculation, i.e., the value at odd spin is larger than the one at even spin. Similarly, the calculated $B(M1)_{\rm in}/B(M1)_{\rm out}$ ratios also reproduce the experimental magnitude, staggering and the trend pattern quite well.

In comparison with Ref. [19], one can draw the conclusion that after including the pairing correlation, not only the energy spectra but also the electromagnetic transition ratios can be well reproduced by the two quasi-particles coupled with a triaxial rotor model.

The lifetime measurement is critical for the identification of chiral bands. So far, no experimental lifetime data are available for the candidate chiral bands in ^{126}Cs. In the present work, the reduced $B(M1)$ and $B(E2)$ transition probabilities are calculated and presented in Fig. 4. The upper panel shows the $B(E2)$ transition probabilities, and the lower panel corresponds to the $B(M1)$ transition probabilities. At low spins, the intraband and interband $B(E2)$ transition probabilities are close to each other. After $I = 13\hbar$, the intraband $B(E2)$ values steadily increase with spin, whereas interband $B(E2)$ values steeply decrease and vanish for $I \geq 15\hbar$. It is noted that both the intraband $B(E2)$ values for the two bands are very similar, which is consistent with the ideal chiral criteria. The calculated $B(M1)$ values in the lower panel of the Fig. 4 show remarkable odd-even staggering. The intraband $B(M1)$ values at odd spin are larger than the values at even spin, which has opposite phase with the staggering in the interband $B(M1)$ values. The staggering amplitude in interband $B(M1)$ transitions is larger than in the intraband $B(M1)$ transitions. From Fig. 4, it is clear that the staggering of the $B(M1)/B(E2)$ ratios is attributed to the staggering of the $B(M1)$ values.

To further confirm the picture of the chirality in ^{126}Cs, the orientation of the angular

momentum for the rotor as well as the valence proton and neutron are investigated and shown in Fig. 5. As in Ref. [7], the effective angle $\theta_{\rm PN}$ between the angular momenta of the proton $\mathbf{j}_{\rm p}$ and the neutron $\mathbf{j}_{\rm n}$ is defined as, $\cos\theta_{\rm PN} = \langle \mathbf{j}_{\rm p} \cdot \mathbf{j}_{\rm n} \rangle / \sqrt{\langle j_{\rm p}^2 \rangle \langle j_{\rm n}^2 \rangle}$. Similarly, one can define the effective angle $\psi_{\rm RP}$ ($\psi_{\rm RN}$) between the angular momenta of the core and the valence proton (neutron). The results of the effective angles are shown in Fig. 5. In the spin interval $9\hbar \leq I \leq 15\hbar$, the values of three effective angles are larger than 45°, which indicates a remarkable aplanar rotation in this nucleus. This provides additional support for the existence of chiral bands in ^{126}Cs.

IV. SUMMARY

In summary, the positive parity doublet bands in ^{126}Cs based on the $\pi h_{11/2} \otimes \nu h_{11/2}$ configuration have been studied by using the two quasi-particles plus a triaxial rotor model. The energy spectra, energy staggering parameter $S(I)$, the intraband $B(M1)/B(E2)$ and the $B(M1)_{\rm in}/B(M1)_{\rm out}$ are calculated and compared with the available experimental data. After including the pairing correlation, not only the energy spectra but also the electromagnetic transition ratios can be well reproduced by the two quasi-particles coupled with a triaxial rotor model, which supports the existence of chiral bands in this nucleus. The absolute $B(M1)$ and $B(E2)$ transition probabilities have been presented which is supposed to invite future experiment on lifetime measurement. The chiral interpretation of this doublet bands in ^{126}Cs is also supported by the effective angles between the angular momenta of the core, valence proton and neutron. The success of the present two quasi-particles plus a triaxial rotor model indicates the necessity for a multi-proton and neutron plus a triaxial rotor model which is in progress.

This work is partly supported by the National Natural Science Foundation of China under Grant No. 10605001, 10435010, 10221003, and 10505002.

[1] S. Frauendorf and J. Meng, Nucl. Phys. **A617**, 131 (1997).

[2] K. Starosta *et al.,* Phys. Rev. Lett. **86**, 971 (2001).

[3] T. Koike, K. Starosta, C.J. Chiara, D.B. Fossan, and D.R. LaFosse, Phys. Rev. C **63**, 061304(R) (2001).

[4] D.J. Hartley *et al.,* Phys. Rev. C **64**, 031304(R) (2001).

[5] A.A. Hecht *et al.,* Phys. Rev. C **63**, 051302(R) (2001).

[6] R.A. Bark, A.M. Baxter, A.P. Byrne, G.D. Dracoulis, T. Kibedi, T.R. McGoram, and S.M. Mullins, Nucl. Phys. **A691**, 577 (2001).

[7] K. Starosta, C. J. Chiara, D. B. Fossan, T. Koike, T. T. S. Kuo, D. R. LaFosse, S. G. Rohozinski, Ch. Droste, T. Morek and J. Srebrny Phys. Rev. C **65**, 044328 (2002).

[8] X.F. Li *et al.,* Chin. Phys. Lett. **19**, 1779 (2002).

[9] T. Koike, K. Starosta, C.J. Chiara, D.B. Fossan, and D.R. LaFosse, Phys. Rev. C **67**, 044319 (2003).

[10] G. Rainovski *et al.,* Phys. Rev. C **68**, 024318 (2003)

[11] C. Vaman, D.B. Fossan, T. Koike, K. Starosta, I.Y. Lee and A.O. Macchiavelli, Phys. Rev. Lett. **92**, 032501 (2004).

[12] P. Joshi *et al.,* Phys. Lett. **B595**, 135 (2004).

[13] Shouyu Wang, Yunzuo Liu, T. Komatsubara, Yingjun Ma, and Yuhu Zhang, Phys. Rev. C **74**, 017302 (2006).

[14] D. Tonev *et al.,* Phys. Rev. Lett. **96**, 052501 (2006).

[15] C.M. Petrache, G.B. Hagemann, I. Hamamoto and K. Starosta, Phys. Rev. Lett. **96**, 112502 (2006).

[16] E. Grodner *et al.*, Phys. Rev. Lett. **97**, 172501 (2006).

[17] V.I. Dimitrov, S. Frauendorf, and F. Dönau, Phys. Rev. Lett. **84**, 5732 (2000).

[18] S. Frauendorf, Rev. Mod. Phys. **73**, 463 (2001).

[19] J. Peng, J. Meng, S. Q. Zhang, Phys. Rev. C **68**, 044324 (2003).

[20] J. Peng, J. Meng, S. Q. Zhang, Chin. Phys. Lett. **20**, 1223 (2003).

[21] T. Koike, K. Starosta and I. Hamamoto, Phys. Rev. Lett. **93**, 172502 (2004).

[22] P. Olbratowski, J. Dobazewski, J. Dudek, and W. P*ló*ciennik, Phys. Rev. Lett. **93**, 052501 (2004).

[23] P. Olbratowski, J. Dobazewski and J. Dudek, Phys. Rev. C **73**, 054308 (2006).

[24] J. Meyer-ter-vehn, Nucl. Phys. **A249**, 111 (1975).

[25] I. Ragnarsson and P.B. Semmes, Hyperfine Interaction **43**, 425 (1988).

[26] S. Q. Zhang, B. Qi, S. Y. Wang, and J. Meng, to be submitted.

[27] N. Tajima, Nucl. Phys. **A572**, 265 (1994).

[28] M.S. Fetea, V. Nikolova and B. Crider, J. Phys. G **31**, s1847 (2005).

[29] T. Koike *et al.,* FNS2002, Berkeley, CA, 2002, AIP Conf. Proc. No. **656**, edited by P. Fallon and R. Clark (AIP, Melville, New York, 2003), p. 160.

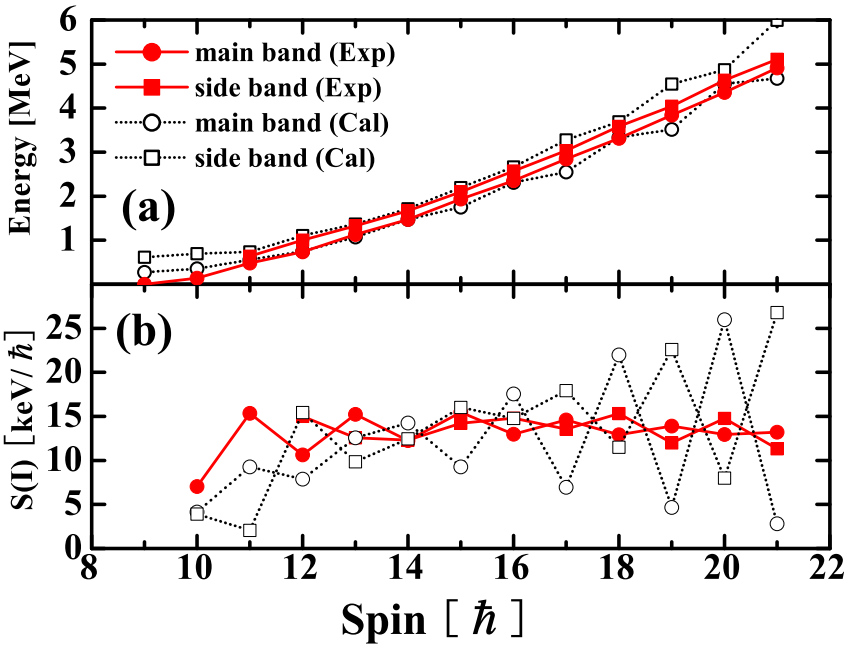

FIG. 1: (Color online) The excitation energy (top panel) and staggering $S(I) = [E(I) - E(I-1)]/2I$ (bottom panel) as a function of spin for the main and side band in ^{126}Cs. The filled (open) symbols connected by solid (dotted) lines are for the experimental (theoretical) values. The main and side band are shown by circles and squares, respectively. The theoretical values in the upper panel are shifted by -2.65 MeV in order to coincide with the experimental energy at $I = 14\ \hbar$.

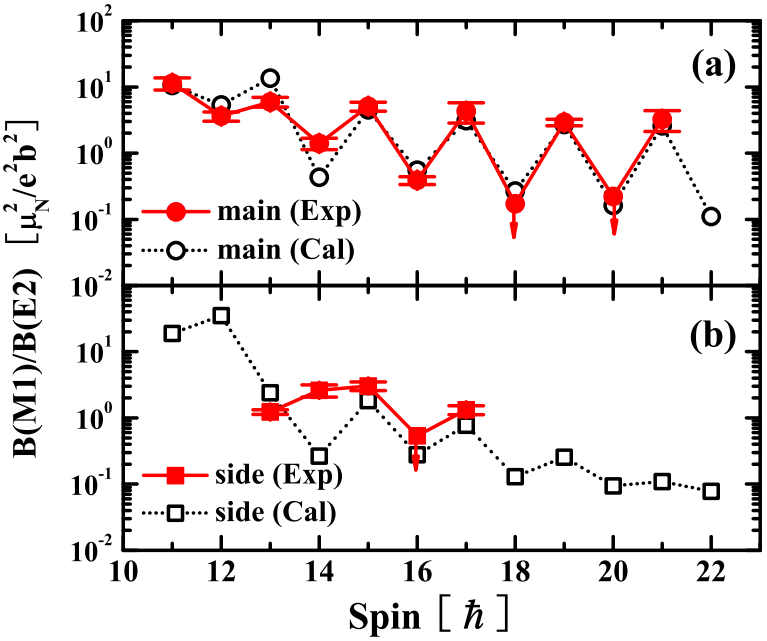

FIG. 2: (Color online) Comparisons between the calculated $B(M1)/B(E2)$ and data available for the main and side band in ^{126}Cs.

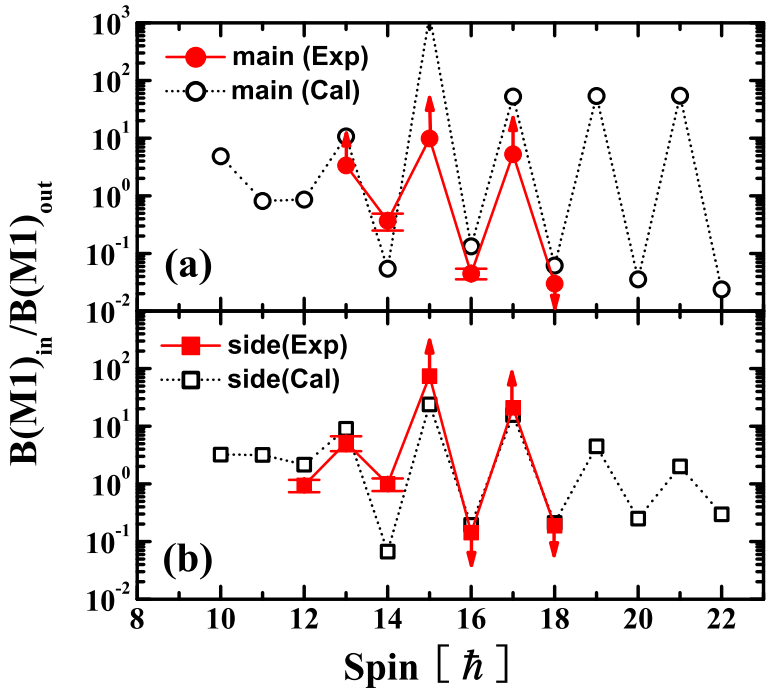

FIG. 3: (Color online) Comparisons between the calculated $B(M1)_{in}/B(M1)_{out}$ and data available for the main and side band in ^{126}Cs.

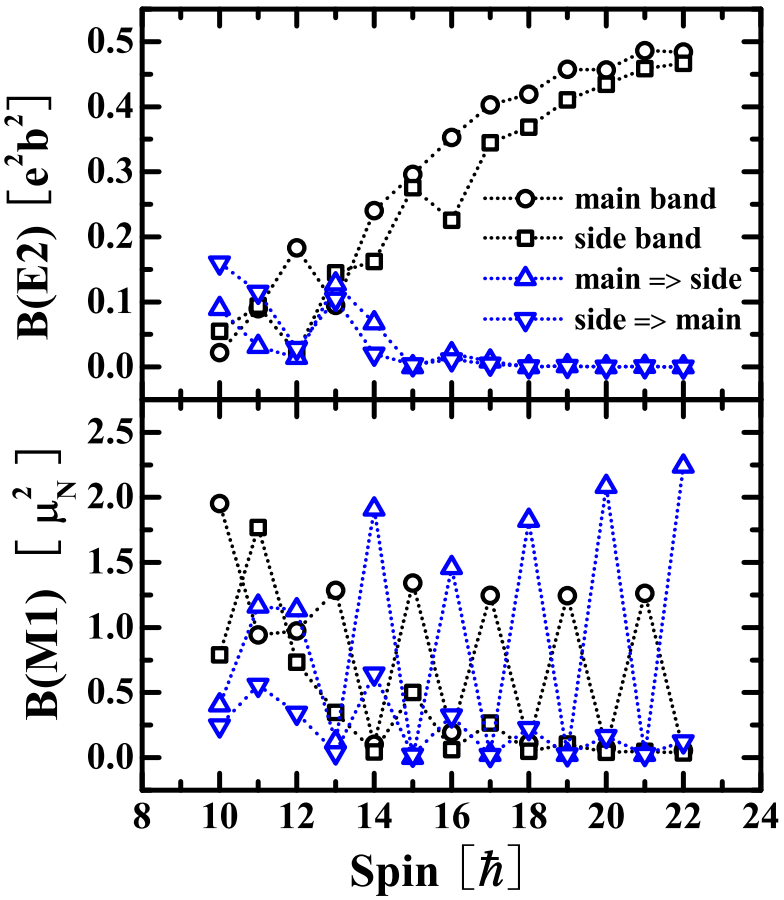

FIG. 4: (Color online) The calculated $B(E2)$ and $B(M1)$ values as functions of the spin in ^{126}Cs. The symbols, circles, squares, triangle ups and triangle downs represent the intraband transitions of the main band, the intraband transitions of the side band, the interband transitions from the main band to the side band, and the interband transitions from the side band to main band, respectively.

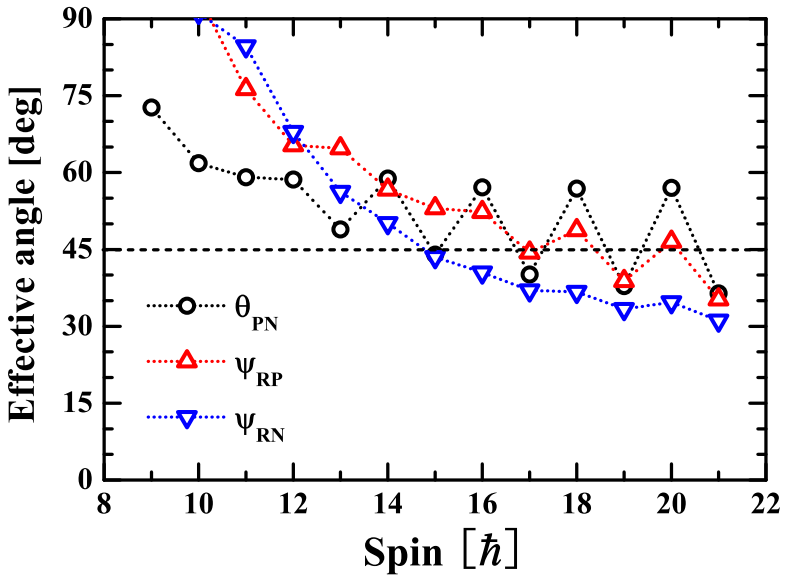

FIG. 5: (Color online) The effective angles $\theta_{\rm PN}$ (circles), $\psi_{\rm RP}$ (triangle ups) and $\psi_{\rm RN}$ (triangle downs) as a function of spin for the main band in ^{126}Cs.